Nuclear Engineering and Technology 55 (2023) 1218–1224

Contents lists available at ScienceDirect

Nuclear Engineering and Technology

journal homepage: www.elsevier.com/locate/net

Original Article

Correlation between the concentration of TeO_2 and the radiation shielding properties in the TeO_2–MoO_3–V_2O_5 glass system

Y. Al-Hadeethi [a, *], M.I. Sayyed [b, c]

[a] Department of Physics, Faculty of Science, King Abdulaziz University, Jeddah, 21589, Saudi Arabia
[b] Department of Physics, Faculty of Science, Isra University, Amman, Jordan
[c] Department of Nuclear Medicine Research, Institute for Research and Medical Consultations (IRMC), Imam Abdulrahman Bin Faisal University, P.O. Box 1982, Dammam, 31441, Saudi Arabia

ARTICLE INFO

Article history:
Received 10 October 2022
Received in revised form
8 December 2022
Accepted 11 December 2022
Available online 13 December 2022

Keywords:
Mass attenuation coefficients
Glasses
TeO_2
Phy-X software

ABSTRACT

We investigated the radiation shielding competence for TeO_2–V_2O_5–MoO_3 glasses. The Phy-X software was used to report the radiation shielding parameters for the present glasses. With an increase in TeO_2 and MoO_3 content, the samples' linear attenuation coefficient improves. However, at low energies, this change is more apparent. At low energy, the present samples have an effective atomic number (Z_{eff}) that is relatively high (in order of 16.17–24.48 at 0.347 MeV). In addition, the findings demonstrated that the density of the samples is a very critical factor in determining the half value layer (HVL). The minimal HVL for each sample can be found at 0.347 MeV and corresponds to 1.776, 1.519, 1.391, 1.210 and 1.167 cm for Te1 to Te5 respectively. However, the highest HVL of these glasses is recorded at 1.33 MeV, which corresponds to 3.773, 3.365, 3.218, 2.925 and 2.908 cm respectively. The tenth value layer results indicate that the thickness of the specimens needs to be increased in order to shield the photons that have a greater energy. Also, the TVL results demonstrated that the sample with the greatest TeO_2 and MoO_3 concentration has a higher capacity to attenuate photons.

1. Introduction

Our knowledge of radiation science has quickly advanced over the past century, which has resulted in the proliferation of nuclear engineering applications. The establishment of such technologies carries with it an obvious disadvantage, which results from the inadequacy of the safeguards taken against the ionizing radiation caused by the operation of the devices and the usage of radioactive sources [1–3]. Gamma rays are an example of an ionizing radiation type. This form of radiation is produced when an unstable nucleus emits photons. Radioactive isotopes may be put to a variety of beneficial purposes in our day-to-day lives, spanning from the exploitation of the radiation in medical settings to applications in the agricultural and industrial sectors [4–7]. An excessive amount of radiation exposure can have negative impacts on a person's health, including nausea, exhaustion, vomiting, and even possible death. It will be vital to construct structures that are resistant to the negative effects of radiation on humanity as nuclear sectors develop further. This is because radiation may cause cancer and other diseases. To reduce the likelihood of occurrences that might result in a loss of control over nuclear plants, it is essential to put in place sufficient radiation shielding measures and a comprehensive set of preventative health and safety protocols [8–11]. Accidents involving nuclear power, such as the one that occurred at Chernobyl, will continue to cause harm to people and be a source of danger so long as new materials with superior radiation shielding qualities are not developed. The proper design of radiation shielding materials is essential in order to meet the requirements for reducing the dangers associated with ionizing radiation exposure. The currently available techniques of shielding are unsustainable because of the high expenses involved and the potential risk to human health that they pose. Lead sheets are a good example of a material that is functional but harmful. As a result, as a replacement for products that include lead, special protective materials that are harmless, friendly to the environment, and inexpensive need to be produced [12–16]. Materials that consist of a high atomic number (Z) are good choices due to their capacity to interact with radiation. Glass, for instance, is among the most often utilized materials in the nuclear sector due to the material's favorable features. This is because glasses are ecologically benign,

* Corresponding author.
E-mail address: yalhadeethi@kau.edu.sa (Y. Al-Hadeethi).

https://doi.org/10.1016/j.net.2022.12.014

have cheap production costs, can be made denser by adding heavy elements and are transparent -protective layers [17–20]. Due to its use in thermoluminescent dosimeters, scintillators, solar cells, laser technology, and gamma radiation detectors, research on diverse glass systems has become more popular. Tellurite glasses have received attention as the need for superior glass systems for modern technological purposes intensifies. TeO_2 glasses exhibit noteworthy physical features such as good thermal and chemical stability, low phonon energy, high refractive index, good devitrification resistance, and low melting temperature. Because of their exceptional properties, tellurite glasses are considered promising materials for a variety of optical applications as well as applications involving radiation shielding. Recent research has shown that tellurite glasses have potential shielding qualities that are on equivalent with or perhaps superior to those offered by other types of glass systems [20,21]. Because of this, having a knowledge of the shielding efficiency of tellurite-based glasses as well as their capacity to lower the intensity of radiation exposure has become very necessary in order to be capable of utilizing these glasses in an environment that is contaminated with radiation [22,23]. In light of this, the purpose of this study is to analyze the radiation shielding capabilities of TeO_2–V_2O_5–MoO_3 glasses in order to assess their possibility for use in applications involving the shielding of gamma rays.

2. Materials and methods

It is general information that the gamma-ray shielding properties of any material are determined by both the substance's composition and its density. The mass attenuation coefficient (MAC, or μ/ρ) may be calculated for multi-component specimens (like the tested TeO_2–V_2O_5–MoO_3 glasses) by utilizing Equation (1):

$$(\mu/\rho)_{glass} = \sum_i w_i (\mu/\rho)_i \quad (1)$$

In the formula shown above, the $(\mu/\rho)_i$ represents the MAC for the following elements: O, V, Mo and Te. While the w_i is the weight fractions of the aforementioned elements in each sample. In addition, there is a parameter known as the linear attenuation coefficient (LAC, or μ), which gives information about the percentage of gamma photons that are reduced after entering a medium. Usually, it is measured in a unit of 1/cm or 1/mm. It is a parameter that depends on density as well as on energy. The preceding parameter is significant since it contributes to the determination of many other shielding variables, for example the half value layer (HVL). HVL refers to the thickness of the barrier at the point at which fifty percent of the photons have been reduced. HVL is photon energy-dependent, like LAC. For the purpose of determining the HVL of any given attenuator, the next formula is applied:

$$HVL = \frac{0.693}{\mu} \quad (2)$$

In addition, the mean free path (MFP) can be another component that the inventors of shielding glasses are using to determine the distance that photons move inside the sample between collisions. It is desirable to use a sample that has a short HVL in addition to an MFP for useful uses, particularly in situations where there is limited space. This may be accomplished by utilizing samples with a high density that are rich in heavy metal oxides like TeO_2 and MoO_3. For the purpose of determining the MFP of the TeO_2–V_2O_5–MoO_3 glasses that were tested, the formula given below can be utilized:

$$MFP = \frac{1}{\mu} \quad (3)$$

In addition, we assessed the effective atomic number (Z_{eff}) for the particular TeO_2–V_2O_5–MoO_3 glasses that we had chosen. This is a description of how radiation interacts with composites. High Z_{eff} for the medium indicates that it has a strong capacity to shield the incident radiation. The Z_{eff} is related to basic parameters known as the total atomic and electronic cross sections (σ_T and σ_e). They are given by:

$$\sigma_T = \left(\frac{\sum_i f_i A_i}{N_A}\right)(\mu/\rho) \quad (4)$$

and

$$\sigma_e = \frac{1}{N_A}\sum_i \left[\left(\frac{f_i A_i}{Z_i}\right)(\mu/\rho)\right] \quad (5)$$

here N_A and Zi represent Avogadro's number and the atomic number of the ith element respectively. From these two equations, the Z_{eff} is calculated. Namely:

$$Z_{eff} = \frac{\sigma_T}{\sigma_e} \quad (6)$$

Using the computer PhyX [24], we were able to derive the aforementioned values, which are provided in equation 1 through 6, for the glasses that were tested. This user-friendly online software was produced in 2020, and it can estimate a number of radiation-shielding variables, such as Z_{eff}, in the continuous energy area or for selected energy values. This program is easily accessible to researchers over the internet at https://phy-x.net/PSD. In brief, the following is a description of the procedure that may be used with this program to calculate specific shielding variables for any given sample:

(1) Define the composition and the density of the sample: by selecting the plus sign on the program's main screen, the researcher could simultaneously specify an infinite number of samples.
(2) Selection the energies
(3) Selection of the radiation shielding quantitates to be computed

More details about this software are available in the recent work [24].

The present glasses are selected from Ref. [25] and the following are the description of the composition of these glasses:

Te1: $30TeO_2$–$55V_2O_5$–$15MoO_3$, density = 3.574 g/cm^3

Te2: $40TeO_2$–$40V_2O_5$–$20MoO_3$, density = 4.033 g/cm^3

Te3: $50TeO_2$–$25V_2O_5$–$25MoO_3$, density = 4.246 g/cm^3

Te4: $60TeO_2$–$10V_2O_5$–$30MoO_3$, density = 4.705 g/cm^3

Te5: 66.7TeO_2-33.3MoO_3, density = 4.757 g/cm^3

3. Results and discussion

In order to analyze the attenuation characteristics of the chosen TeO_2–V_2O_5–MoO_3 glasses, we utilized the Phy-X software to derive the values of μ/ρ. This allowed us to examine the attenuation features of the present system. The range of energies that was looked at for this study was from 0.347 MeV up to 1.33 MeV, and the data are presented in Fig. 1. It is clear that the μ/ρ values for all of the samples are greater at 0.347 MeV than they are at the various energies that were taken into consideration for this work. These values are equal to 0.109, 0.113, 0.117, 0.122 and 0.125 cm^2/g for the Te1 to Te5 glasses, respectively. The maximum levels for this variable, which occurred at 0.347 MeV, may be a sign of a higher possibility of photons interacting with TeO_2–V_2O_5–MoO_3 glasses through a photoelectric process.

It is important to note that 0.347 MeV is less than the other selected energies, and it is well known that radiations with lower energies have a greater likelihood of interacting through this mechanism. When the energy is increased from 0.347 to 0.826 MeV, there is a noticeable trend toward rapid declines in the values of μ/ρ (for instance, the μ/ρ for Te1 falls from 0.109 to 0.066 cm^2/g as the energy increases from 0.347 to 0.826 MeV). Further, it has been shown that μ/ρ reduces extremely slowly at higher energy, and this is ascribed to Compton scattering (for Te1, the μ/ρ lowers from 0.066 to 0.055 between 0.826 and 1.173 MeV). This is because Compton scattering causes the μ/ρ to fall very slowly. According to Fig. 1, the TeO_2–V_2O_5–MoO_3 glasses exhibit a rise in their MAC value for E < 0.826 MeV whenever there is an increase in the amount of TeO_2 present. On the other hand, this rise is much more noticeable at lower energies. As an illustration, we looked at how the presence of TeO_2 affected the μ/ρ at two different energies: 0.347 and 1.173 MeV. When the TeO_2 concentration shifts from 30 to 66.7 mol% at the first energy, the μ/ρ value goes up from 0.109 to 0.125 cm^2/g (the difference is 0.016), but the difference between them is just 0.001 at 1.173 MeV.

For the TeO_2–V_2O_5–MoO_3 glasses, the μ values are displayed versus their TeO_2 contents in Fig. 2. It was clear that there was a correlation between the concentration of TeO_2 and the μ. At energies of 0.347 and 0.511 MeV, the rate of growth of μ is very evident, but at the other energies, it grows at a moderate speed. The rationale for why μ is dependent on the amount of TeO_2 in the sample might be attributed to the density. TeO_2 causes a rise in the density of the glasses, which goes from 3.574 to 4.757 g/cm_3, and it is common knowledge that the μ is proportional to the density of the glasses in a linear way. Consequently, the glass sample with the highest density, Te5, also has the largest LAC at all different energies (0.594 cm^{-1} at 0.347 MeV and 0.312 cm^{-1} at 0.826 MeV). In accordance with the Lambert-Beer Law, we saw in this figure that the μ reduces as the energy level rises. This finding is consistent with this important law [26].

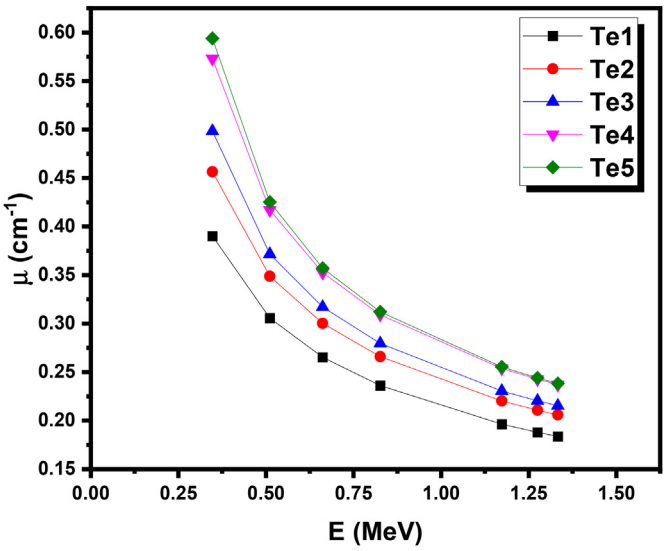

Fig. 2. The linear attenuation coefficient for TeO_2–V_2O_5–MoO_3 glasses.

In order to calculate the effective atomic number (Z_{eff}) of the glasses that were investigated, it was necessary to first determine their σ_T and σ_e values. The data of the total atomic cross-sections (ACS) and total electronic cross-sections (ECS) analyses are presented, respectively, in Fig. 3 and Fig. 4. It is easy to observe from Figs. 3 and 4 that the ACS and ECS values decrease as the energy of the photon increases. Each glass' ACS value is higher than its ECS value.

We were able to figure out the Z_{eff} for TeO_2–V_2O_5–MoO_3 glasses by making use of equation (6), together with the values for ACS and ECS obtained from Figs. 3 and 4.

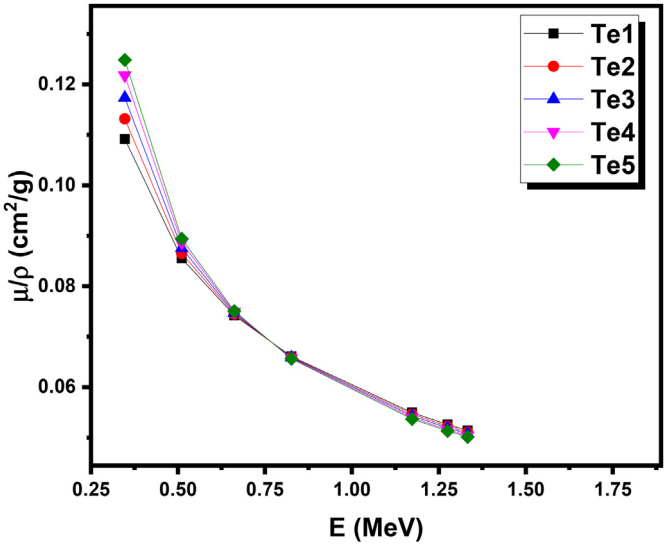

Fig. 1. The mass attenuation coefficient for TeO_2–V_2O_5–MoO_3 glasses.

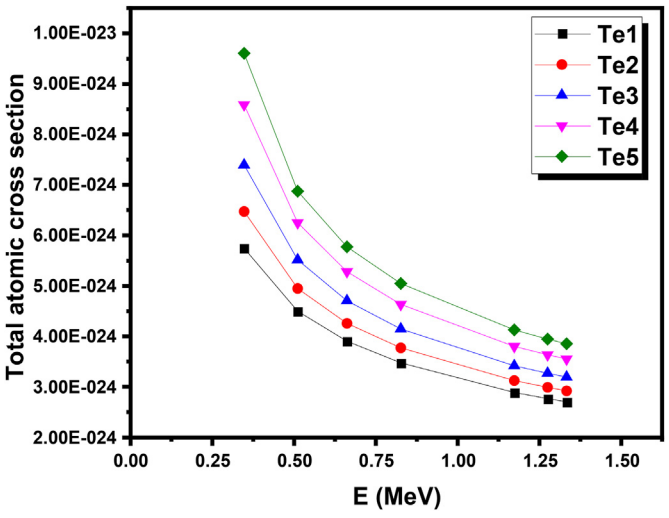

Fig. 3. The total atomic cross section for TeO_2–V_2O_5–MoO_3 glasses.

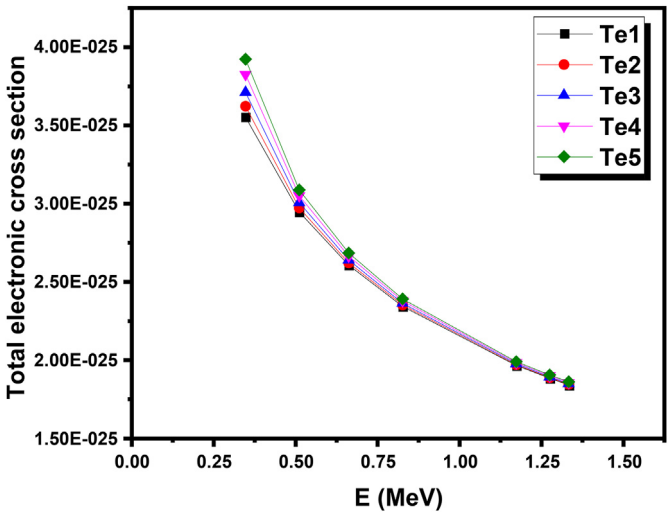

Fig. 4. The total electronic cross section for TeO_2–V_2O_5–MoO_3 glasses.

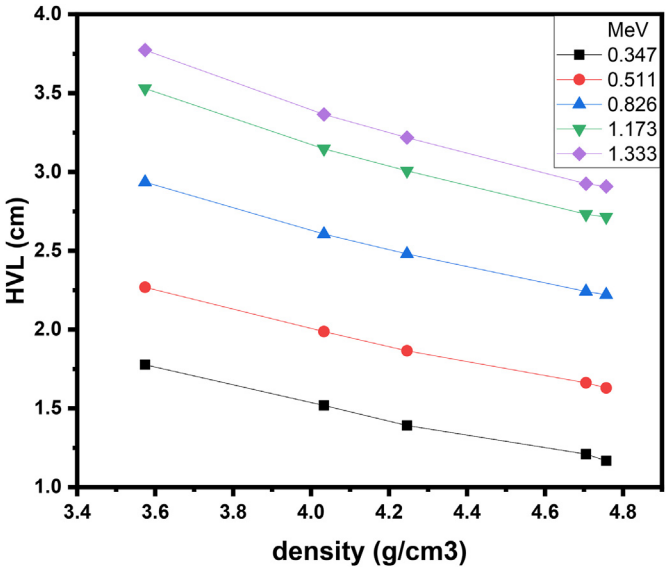

Fig. 6. The half value layer for TeO_2–V_2O_5–MoO_3 glasses.

The Z_{eff} values for the present samples are displayed in Fig. 5 between 0.347 and 1.33 MeV. When it comes to protecting against radiation, a higher Z_{eff} rating indicates that the glass in consideration is superior. According to the figure, the photoelectric effect causes all of the current samples to have a reasonably high Z_{eff} when the energy is minimal. Because the Z_{eff} decreases as the energy level increases, this suggests that the photons have a greater possibility of interacting with the samples while the energy level is lower. According to Fig. 5, the Z_{eff} improved with a greater quantity of TeO_2 across all energies. This can be due to the substitution of V_2O_5 by TeO_2 and MoO_3 (Z for V, Mo and Te is 23, 42 and 52 respectively). The MoO_3 and TeO_2 are responsible for an effective improvement in the Z_{eff}, and this is demonstrated clear when we consider the Te5. If we compare the Z_{eff} for Te1 with this sample (i.e. Te5), we found that the Z_{eff} for Te1 is 16.17 at 0.347 MeV, while it is 24.48 for Te5 at the same energy. For 0.511 MeV, the Z_{eff} for both samples are 15.27 (for Te1) and 22.27 (for Te5). Based on the results that are shown in Z_{eff} figure, we can draw the conclusion that the photons have the least penetrating power when they contact Te5 samples and have the maximum penetrating ability when they connect with Te1 samples correspondingly.

Half value layer, also known as HVL, is one of the most important photon-shielding characteristics of the medium, especially in situations when there is a limited amount of space available. The smaller the HVL, the more advantageous the shielding qualities. Fig. 6 depicts the relationship between the HVL and the sample density. At energies of 0.347 and 0.511 MeV, the HVL drops at a rapid rate with increasing density, however at the other energies, it only declines at a slower rate. This indicates that the density of the specimens has a very crucial influence in the HVL rates, and consequently, the thickness of the specimens that is employed to prevent or reduce the photons. For instance, the HVL of Te4 and Te5 is smaller than that of Te1–Te3 for the same energy because of the difference in the density of these samples. Therefore, a high density of the sample will certainly have an effect on the HVL and will minimize the thickness that is necessary for reducing photons; this

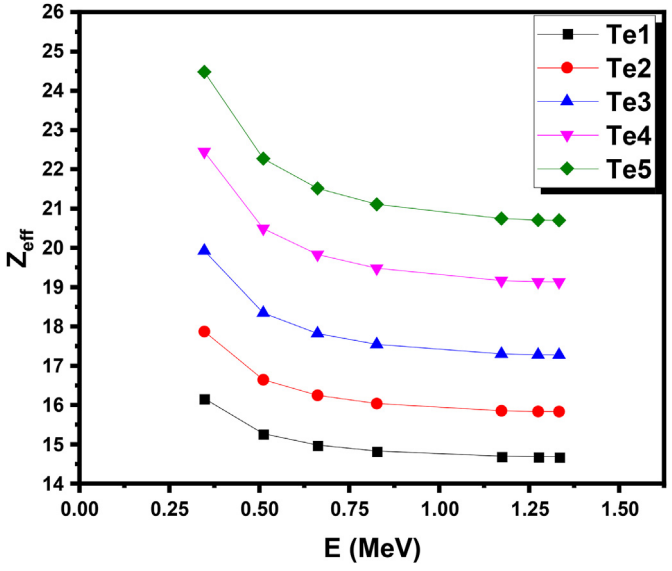

Fig. 5. The effective atomic number for TeO_2–V_2O_5–MoO_3 glasses.

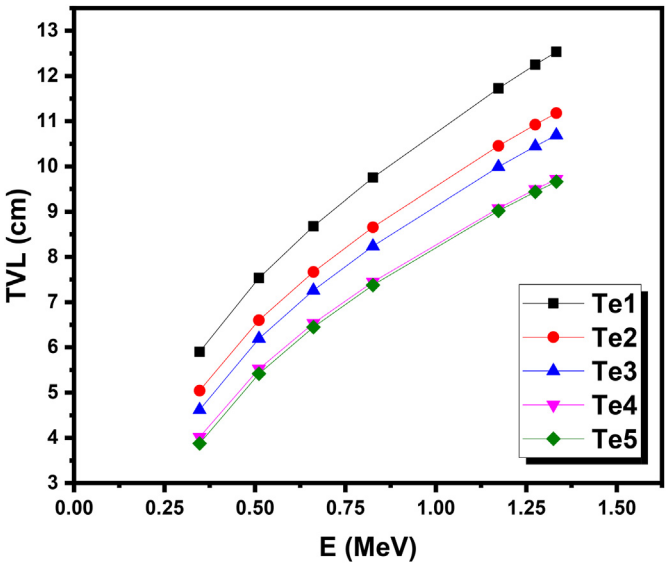

Fig. 7. The tenth value layer for TeO_2–V_2O_5–MoO_3 glasses.

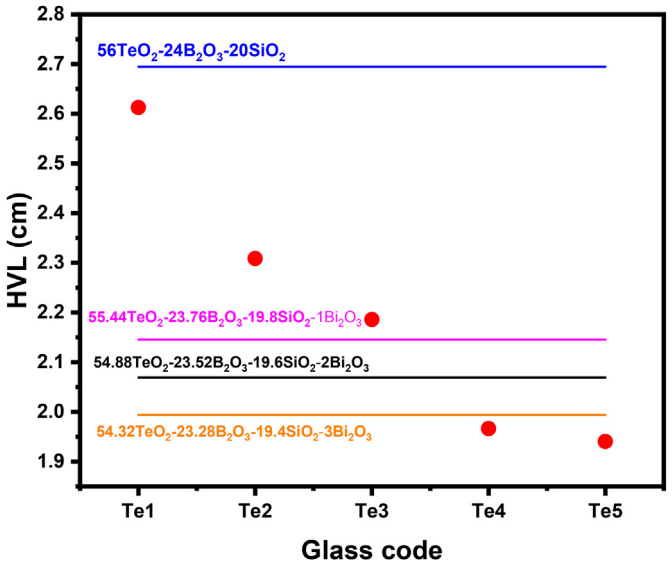

Fig. 8. Comparison between the HVL for the Te1–Te5 glasses with B_2O_3–TeO_2–SiO_2 glasses containing Bi_2O_3.

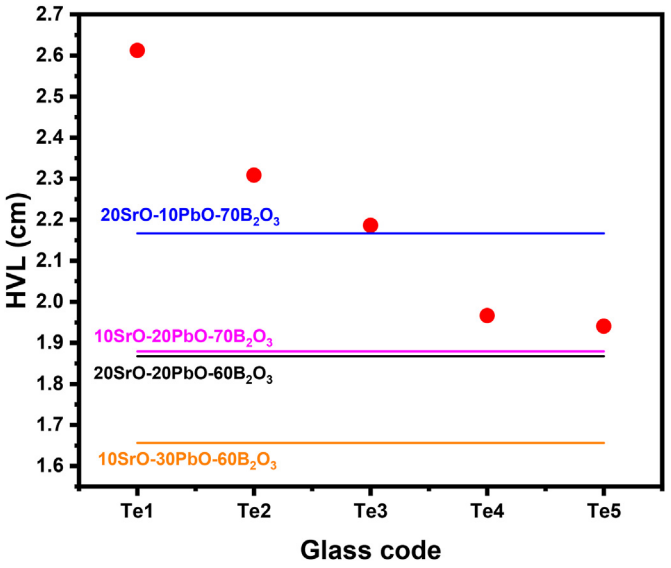

Fig. 10. Comparison between the HVL for the Te1–Te5 glasses with lead strontium borate glasses.

seems to be significant in the event that there is a restricted amount of space available. The minimal HVL for each sample can be found at 0.347 MeV and corresponds to 1.776, 1.519, 1.391, 1.210 and 1.167 cm for Te1 to Te5 respectively. However, the highest HVL of these glasses is recorded at 1.33 MeV, which corresponds to 3.773, 3.365, 3.218, 2.925 and 2.908 cm respectively.

In a manner analogous to that of HVL, we are able to analyze the tenth value layer (TVL). At the energies that were studied, the TVL for the TeO_2–V_2O_5–MoO_3 glasses can be found in Fig. 7. It is clear from looking at this figure that both TVL and HVL are following a similar pattern. Because it is evident that TVL grows with increasing energy, this indicates that the thickness of the specimens needs to be increased in order to shield the photons that have a greater energy. In addition, Fig. 7 demonstrates that there is a downward trend in the TVL when the amount of TeO_2 in the sample increases. The TVL value of Te1 is the highest, while the TVL value of Te5 is the lowest. For example, the TVL for Te1 was 5.901 and 12.534 cm, whereas for Te5 it was only 3.877 and 9.661 cm at the lowest and maximum energy levels, respectively. These data provide further evidence that the sample with the greatest TeO_2 and MoO_3 concentration has a higher capacity to attenuate photons, as was revealed in the earlier curves. The TVL figure indicates that the Te5 sample has the potential to be the most successful candidate for the development of radiation protection glasses.

In Fig. 8, we compared the HVL for the Te1–Te5 glasses at 0.662 MeV with B_2O_3–TeO_2–SiO_2 glasses containing Bi_2O_3 [27]. The HVL for Te1 is about 2.6 cm, whereas it is around 2.7 cm for $56TeO_2$–$24B_2O_3$–$20SiO_2$. Te3 has slightly higher HVL than $55.44TeO_2$-$23.76B_2O_3$-$19.8SiO_2$–$1Bi_2O_3$. Te4 and Te5 samples have close HVL with the B_2O_3–TeO_2–SiO_2 glasses containing 2 and 3 mol% of Bi_2O_3. In Fig. 9, we compared the HVL for the Te1–Te5 glasses at 0.662 MeV with barium boro-vanadate glasses [28]. Te1

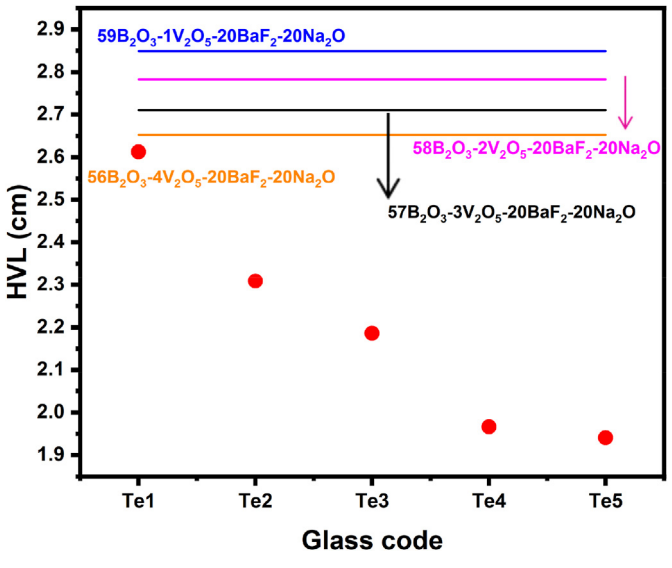

Fig. 9. Comparison between the HVL for the Te1–Te5 glasses with barium boro-vanadate glasses.

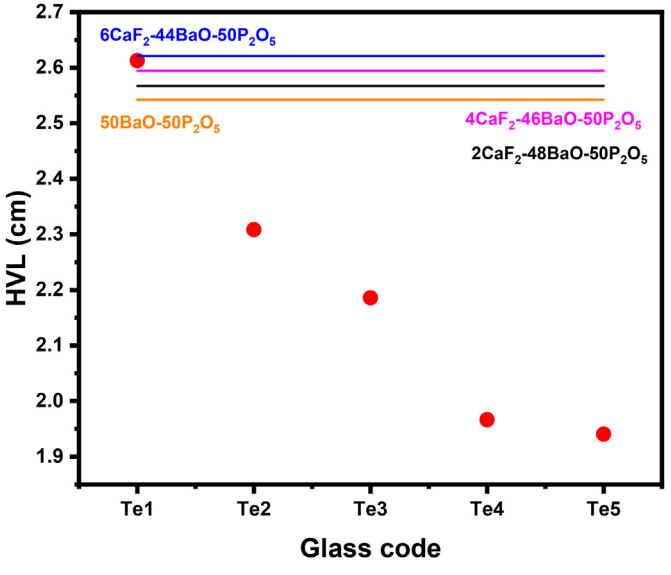

Fig. 11. Comparison between the HVL for the Te1–Te5 glasses with CaF_2–BaO –P_2O_5 glasses.

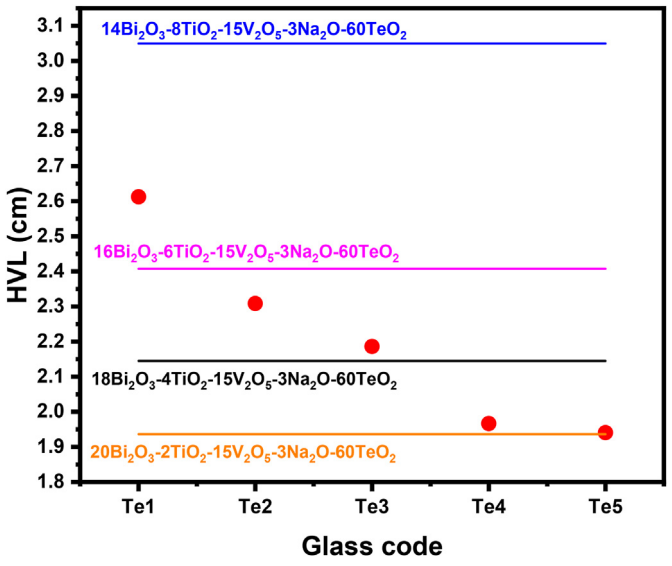

Fig. 12. Comparison between the HVL for the Te1–Te5 glasses with titanium vanadium sodium tellurite glasses.

has close HVL with $56B_2O_3$–$4V_2O_5$–$20BaF_2$–$20Na_2O$ sample, while all the barium boro-vanadate glasses given in Fig. 9 have higher HVL than Te2–Te5 glasses. In Fig. 10, we compared the HVL for the Te1–Te5 glasses at 0.662 MeV with lead strontium borate glasses [29]. Evidently, $20SrO–10PbO–70B_2O_3$ has almost same HVL with Te3, but lower HVL than Te1 and Te2·Te4 and Te5 possess HVL values that are higher than the given lead strontium borate glasses (except $20SrO–10PbO–70B_2O_3$). The comparison between the HVL for the Te1–Te5 glasses with CaF_2–BaO–P_2O_5 glasses is given in Fig. 11 [30]. Only one sample from the CaF_2–BaO–P_2O_5 glasses has close HVL with our glasses (i.e. with Te1), while other CaF_2–BaO–P_2O_5 glasses have much higher HVL than our selected glasses. Fig. 12 represents Comparison between the HVL for the Te1–Te5 glasses with titanium vanadium sodium tellurite glasses [31]. From the titanium vanadium sodium tellurite glasses, the sample with 14 mol% of Bi_2O_3 has much higher HVL than all the Te1–Te5 glasses. Te3 has close HVL with the titanium vanadium sodium tellurite glass sample contains 18 mol% of Bi_2O_3. Te5 has the same HVL with the glass with composition of $20Bi_2O_3$–$2TiO_2$–$15V_2O_5$–$3Na_2O$–$60TeO_2$.

4. Conclusion

In order to report the photons shielding parameters for the TeO_2–V_2O_5–MoO_3 glases, the Phy-X software was utilized. We analyzed the impact of TeO_2 on the μ/ρ at low and high energies and we found that when the TeO_2 concentration shifts from 30 to 66.7 mol% at the first energy, the μ/ρ value goes up from 0.109 to 0.125 cm^2/g (the difference is 0.016), but the difference between them is just 0.001 at 1.173 MeV. At all energies, an increase in TeO_2 content causes a rise in the μ of Te1–Te5 glasses; however, the magnitude of this rise is most pronounced at low energy regions. As a result of a photoelectric phenomenon, the samples which contain different concentrations have a Z_{eff} that is significantly high at low energies. The Z_{eff} for Te1 and Te5 at 0.511 MeV is 15.27 and 22.27. The findings also demonstrated that the density of the samples has a significant impact on the optimal sample thickness for preventing or reducing the transmission of photons. We investigated the relation between the energy of the radiation and the HVL. We found that at energies of 0.347 and 0.511 MeV, the HVL drops at a rapid rate with increasing density, however at the other energies, it only declines at a slower rate. The HVL and TVL results demonstrated that the thickness of the specimens needs to be increased in order to shield the photons that have a greater energy. Also, the HVL and TVL results showed that the sample with the greatest TeO_2 and MoO_3 concentration has a higher capacity to attenuate photons.

Declaration of competing interest

The authors declare that they have no known competing financial interests or personal relationships that could have appeared to influence the work reported in this paper.

Acknowledgement

This research work was funded by Institutional Fund Projects under grant no. (IFPIP: 1495-130-1442). Therefore, authors gratefully acknowledge technical and financial support from the Ministry of Education and King Abulaziz University, DSR, Jeddah, Saudi Arabia.

References

[1] Aljawhara H. Almuqrin, M. I. Sayyed, Radiation shielding characterizations and investigation of TeO2–WO3–Bi2O3 and TeO2–WO3–PbO glasses, Appl. Phys. A 127 (2021) 190.
[2] Mengge Dong, Xiangxin Xue, Yang He, Zhefu Li, Highly cost-effective shielding composite made from vanadium slag and boron-rich slag and its properties, Radiat. Phys. Chem. 141 (2017) 239–244.
[3] Bünyamin Aygün, High alloyed new stainless steel shielding material for gamma and fast neutron radiation, Nucl. Eng. Technol. 52 (2020) 647–653.
[4] Ashok Kumar, D.K. Gaikwad, Shamsan S. Obaid, H.O. Tekin, O. Agar, M.I. Sayyed, Experimental studies and Monte Carlo simulations on gamma ray shielding competence of $(30+x)PbO$-$10WO_3$-$10Na_2O$–$10MgO$–$(40-x)B_2O_3$, Prog. Nucl. Energy 119 (2020) 103047.
[5] Mengge Dong, Xiangxin Xue, Yang He, Liu Dong, Chao Wang, Zhefu Li, A novel comprehensive utilization of vanadium slag: as gamma ray shielding material, J. Hazard Mater. 318 (2016) 751–757.
[6] Shams A.M. Issa, M.I. Sayyed, M.H.M. Zaid, K.A. Matori, Photon parameters for gamma-rays sensing properties of some oxide of Lanthanides, Results Phys. 9 (2018) 206–210.
[7] Y. Al-Hadeethi, M.I. Sayyed, BaO–Li_2O–B_2O_3 glass systems: potential utilization in gamma radiation protection, Prog. Nucl. Energy 129 (2020), 103511.
[8] G. Lakshminarayana, Ashok Kumar, H.O. Tekin, Shams A.M. Issa, M.S. Al-Buriahi, M.G. Dong, Dong-Eun Lee, Jonghun Yoon, Taejoon Park, In-depth survey of nuclear radiation attenuation efficacies for high density bismuth lead borate glass system, Results Phys. 23 (2021), 104030.
[9] Bünyamin Aygün,"Neutron and gamma radiation shielding Ni based new type super alloys development and production by Monte Carlo Simulation technique." Radiat. Phys. Chem. 188 (2021): 109630.
[10] M.I. Sayyed, M.G. Dong, H.O. Tekin, G. Lakshminarayana, M.A. Mahdi, Comparative investigations of gamma and neutron radiation shielding parameters for different borate and tellurite glass systems using WinXCom program and MCNPX code, Mater. Chem. Phys. 215 (2018) 183–202.
[11] Shams A.M. Issa, Mahmoud Ahmad, H.O. Tekin, Yasser B. Saddeek, M.I. Sayyed, Effect of Bi2O3 content on mechanical and nuclear radiation shielding properties of Bi2O3-MoO3-B2O3-SiO2-Na2O-Fe2O3 glass system, Results Phys. 13 (2019), 102165.
[12] I.S. Mahmoud, Shams A.M. Issa, Yasser B. Saddeek, H.O. Tekin, Ozge Kilicoglu, T. Alharbi, M.I. Sayyed, T.T. Erguzel, Reda Elsaman, Gamma, neutron shielding and mechanical parameters for lead vanadate glasses, Ceram. Int. 45 (2019) 14058–14072.
[13] G. Lakshminarayana, Ashok Kumar, H.O. Tekin, Shams A.M. Issa, M.S. Al-Buriahi, M.G. Dong, Dong-Eun Lee, Jonghun Yoon, Taejoon Park, Probing of nuclear radiation attenuation and mechanical features for lithium bismuth borate glasses with improving Bi2O3 content for B2O3 + Li2O amounts, Results Phys. 25 (2021), 104246.
[14] Aslı Araz, Esra Kavaz, Rıdvan Durak, Neutron and photon shielding competences of aluminum open-cell foams filled with different epoxy mixtures: an experimental study, Radiat. Phys. Chem. 182 (2021), 109382.
[15] A.S. Abouhaswa, Esra Kavaz, Bi2O3 effect on physical, optical, structural and radiation safety characteristics of B2O3-Na2O-ZnO-CaO glass system, J. Non-Cryst. Solids 535 (2020), 119993.
[16] B. Aygün, E. Sakar, O. Agar, M.I. Sayyed, A. Karabulut, V.P. Singh, Development of new heavy concretes containing chrome-ore for nuclear radiation shielding applications, Prog. Nucl. Energy 133 (2021), 103645.
[17] Y. Al-Hadeethi, S.A. Tijani, The use of lead-free transparent 50BaO-(50-x) borosilicate-xBi_2O_3 glass system as radiation shields in nuclear medicine,

J. Alloys Compd. 803 (2019) 625–630.
[18] M.I. Sayyed, K.A. Mahmoud, Simulation of the impact of Bi2O3 on the performance of gamma-ray protection for lithium zinc silicate glasses, Optik 257 (2022) 168810.
[19] M.I. Sayyed, I.A. El-Mesady, A.S. Abouhaswa, A. Askin, Y.S. Rammah, Comprehensive study on the structural, optical, physical and gamma photon shielding features of B2O3-Bi2O3-PbO-TiO2 glasses using WinXCOM and Geant4 code, J. Mol. Struct. 1197 (2019) 656–665.
[20] R. El-Mallawany, M.I. Sayyed, Comparative shielding properties of some tellurite glasses: Part 1, Phys. B Condens. Matter 539 (2018) 133–140.
[21] Aljawhara H. Almuqrin, Hanfi Mohamed, K.G. Mahmoud, M.I. Sayyed, Hanan Al-Ghamdi, Dalal Abdullah Aloraini, The role of La2O3 in enhancement the radiation shielding efficiency of the tellurite glasses: monte-carlo simulation and theoretical study, Materials 14 (2021) 3913, https://doi.org/10.3390/ma14143913.
[22] M. Çelikbilek, A.E. Ersundu, S. Aydin, Glass Formation and characterization studies in the TeO_2-WO_3-Na_2O system, J. Am. Ceram. Soc. 96 (2013) 1470–1476.
[23] Y.S. Rammah, F.I. El-Agwany, K.A. Mahmoud, A. Novatski, R. El-Mallawany, Role of ZnO on TeO2. Li2O. ZnO glasses for optical and nuclear radiation shielding applications utilizing MCNP5 simulations and WINXCOM program, J. Non-Cryst. Solids 544 (2020), 120162.
[24] Erdem Şakar, Özgür Fırat Özpolat, Bünyamin Alım, M.I. Sayyed, Murat Kurudirek, Phy-X/PSD: development of a user friendly online software for calculation of parameters relevant to radiation shielding and dosimetry, Radiat. Phys. Chem. 166 (2020), 108496.
[25] Tina Tasheva, Vesselin Dimitrov, Correlation between structure and optical basicity of glasses in the TeO2-V2O5-MoO3 system, J. Non-Cryst. Solids 570 (2021), 120981.
[26] V. Mosorov, The Lambert-Beer law in time domain form and its application, Appl. Radiat. Isot. 128 (2017) 1–5.
[27] I.G. Geidam, K.A. Matori, M.K. Halimah, K.T. Chan, F. Muhammad, M. Ishak, S.A. Umar, Oxide ion polarizabilities and gamma radiation shielding features of TeO2–B2O3–SiO2 glasses containing Bi2O3 using Phy-X/PSD software, Mater. Today Commun. 31 (2022), 103472 ().
[28] A. Abouhaswa, F.I. El-Agawany, E.M. Ahmed, Y.S. Rammah, Optical, magnetic characteristics, and nuclear radiation shielding capacity of newly synthesized barium boro-vanadate glasses: B2O3–BaF2–Na2O–V2O5, Radiat. Phys. Chem. 192 (2022), 109922 ().
[29] R.S. Kaundal, Sandeep Kaur, Narveer Singh, K.J. Singh, Investigation of structural properties of lead strontium borate glasses for gamma-ray shielding applications, J. Phys. Chem. Solid. 71 (2010) 1191–1195.
[30] Y. Al-Hadeethi, M.I. Sayyed, Evaluation of gamma ray shielding characteristics of CaF2–BaO –P2O5 glass system using Phy-X/PSD computer program, Prog. Nucl. Energy 126 (2020), 103397.
[31] M.H.M. Zaid, K.A. Matori, H.A.A. Sidek, I.R. Ibrahim, Bismuth modified gamma radiation shielding properties of titanium vanadium sodium tellurite glasses as a potent transparent radiationresis.